

ARIES-ADA Topical Workshop



Scintillation Screens and Optical Technology for transverse Profile Measurements

Krakow, Poland, April 1 to 3, 2019

INDICO-site: <https://indico.cern.ch/event/765975/>

Workshop Summary

Editors: Enrico Bravin, Peter Forck, Ubaldo Iriso, Rhodri Jones, Gero Kube, Thibaut Lefevre, Beata Walasek-Höhne, Adriana Wawrzyniak



Organized by:   and   

Sponsored by:        

This project has received funding from the European Union’s Horizon 2020 programme under Grant Agreement No 730871

Session 1: Scintillator Physics and Technology (P. Forck)

Profile Measurements with Scintillators: Requirements and application at accelerators

Gero Kube, DESY, Hamburg, Germany

The talk serves as an overview concerning the usage of scintillation screens at accelerators for transverse profile determination. The general scheme, namely the insertion of a scintillator disk and the observation with a camera was applied from the beginning of accelerator development and seems to be very simple technology. The light is generated close to the beam particle's trajectory, which results in a beam image. However, scintillation is a multi-step process starting with the generation of fast electrons by the primary beam interaction, followed by thermalization of the electrons and the capture in luminescence centres.

For high energetic beams the primary collision can result in a high velocity of the first stage electrons, which has to be considered in case of high resolution small beam detection. For an ion impact, the ionization density might be very high (compared to the typical usage for medical imaging or for HEP experiments); a summarizing comparison of typical properties for medical and HEP applications compared to the beam instrumentation usage is given in the last slide. A collection of typically scintillator material is given and their properties are summarized. Detailed test of various materials at MAMI and DESY are depicted and compared to OTR measurements. Results obtained at XFEL are shown, the so called 'smoke rings', but are discussed in more detail in a second talk by the author.

The resolution limits by the optics setup and in particular by the observation geometry are given in terms of an overview using instructive plots, more details on the limiting factors are discussed in several other talks.

Introduction to scintillator physics

Weronika Wolszczak, Delft University of Technology, Netherlands

The subject of the talk is a general introduction to the physics of the scintillation process: As a first step by the primary particle interaction, fast electrons are liberated, which then collide with the electrons in the conducting band leading to a thermalization. The slowed down electrons are then captured to either traps or luminescence centres by impurities or crystal defect. The observed light in the optical region is then emitted by the spontaneous decay of these excited states. The holes created by the primary beam interaction thermalize as well and serve as the partner for the exciton generation.

The properties of the intrinsic scintillator type (like NaCl, KCl and KBr), based on exciton or colour centre emission is discussed in terms of emission and absorption wavelength. The importance of self-trap excitons is pointed out together with their temperature dependence, which can be reduced by a factor 10 between LN₂ and room temperature. For doped scintillators the emission properties can be quite different as they are greatly influenced on the doping species; as an example the emission wavelength for various types is discussed as well as their temperature dependence.

To model the generation of luminescence centres, the interaction of the primary particle has to be considered to estimate the ratio of exciton and self-trapped hole generation compared to the dopant excitation. This is important to model any non-proportionality (i.e. a non-linear behaviour between the deposited energy by the primary particle and the light output). Examples for different scintillators are discussed for γ and electron impact. This leads to different densities of the ionization along the primary particle trajectory with a radius up to the 100 nm range and include significant time dependences. The effect can be simulated by Monte-Carlo methods and it is shown that it depends on the primary electron energy with a different scaling for the various materials; the effect was explained in the talk (and is of importance for the usage as beam instrumentation). The related experimental techniques are briefly summarized.

Usage and technology of fast scintillators

Etiennette Auffray, CERN, Geneva, Switzerland

The motivation of this talk is related to the requirements of High Energy Physics detectors like of CERN's CMS and LHCb in terms of high rate capability and radiation hardness. A fast decay time of the scintillator is required to distinguish between different hits and enable high spatial resolving track reconstruction. But also for medical PET tomography the fast timing properties enable a more precise reconstruction by efficient background reduction. The related properties of the scintillator are discussed; beside a fast decay time, a large amount of photons increases the accuracy of the arrival time determination. Additionally, the scintillator geometry and the photo detector time response can be optimized.

The scintillator properties can be influenced by the doping ions; this is discussed for the case of YAG:Ce using the technique of co-doping with an addition of e.g. Mg to the main Ce doping (e.g. to decrease the afterglow contribution). The light transport with respect to timing issues are discussed with nano-structural modification of the crystal surface. The timing properties of different scintillators are compared and design criteria for fast timing achievements are given. The application for calorimeters at HEP detectors and PET scanners are discussed.

Radiation damage is a further challenge for HEP detectors. The creating of traps leads to a decrease of light yield as the electrons or holes are captured as a competing process to the original luminescence levels. Moreover, the absorption increases by transitions to the trap levels. It is shown that a certain recovery of damage occurs with pronounced temperature dependences. The radiation hardness is influenced by the dopant as a comparison of garnets shows. The related parameters of scintillating fibres are discussed as well showing the progress obtained in the last years. A recent article summarizes the actual status of the research: C. Dujardin, E. Auffray, E. Bourret-Courchesne, P. Dorenbos, P. Lecoq, M. Nikl, A. N. Vasil'ev, A. Yoshikawa, and R.-Y. Zhu, '*Needs, Trends, and Advances in Inorganic Scintillators*', IEEE Transaction on Nuclear Science, Vol. 65, No. 8, August 2018, page 1977 – 1997.

The talk concluded with the announcement of the conference series SCINT, organized by the experts in inorganic scintillator design, production and usage.

Production and use of inorganic scintillators

Jiri Parizek, CRYTUR, Turnov, Czech Republic

CRYTUR is one of the suppliers for inorganic scintillators, with a tradition dating back to the 1940th as a university institute. Beside the production of standard scintillators, a strong R&D participation in recent developments is the strength of this company. They host the production chain of various type of scintillator (YAG, LuAG, YAP, PWO etc.) with a great variety of dopants.

The production method is discussed showing the different steps to achieve the required quality and homogeneous scintillator size. Quality assurance using typical material characterization methods is a major topic to maintain the high quality production. The properties of screens, as used in beam instrumentation, are discussed showing the feasibility of production of thin screens. In the case of YAG this can be a free-standing versions (down to 50 μm for 50 mm diameter and 20 μm for 10 mm diameter), designs with a ring support or on a substrate (down to 10 μm). Moreover, fibres can be produced. The response to X-rays (10 to 100 keV) and the temperature dependence are shown for different materials as well as results from radiation hardness tests are discussed.

New materials are developed (partly in collaboration with research institutes) like GAAG, CRY19 CRY060 etc. for the optimization of light yield or fast decay time. The corresponding powders are available as well.

Entire systems for X- and γ -ray imaging are produced and an example for the achievable resolution was discussed.

Session 2: Cameras, Optics and Electronics I (E. Bravin)

Introduction to relevant optical technologies and screen resolution & PSF investigations

Stephen Gibson, Royal Holloway University of London, United Kingdom

Acquiring precise images of a particle beam is a difficult task, this presentation illustrates the main challenges and the state of the art methods used in the field.

Beam images are used to extract the beam size, the transverse distribution (profile) and position. First there is the interaction between the beam and a radiator (e.g. scintillating screen, or OTR radiator), then the transport of the light through an optical system, then the raw image is acquired on camera. The camera images may then need post processing in order to remove artefacts introduced by the radiator or the optical system. At the end the real beam distribution is obtained.

The light generated inside scintillators is affected by refraction, so the apparent size of a particle beam depends on the angle of observation and the thickness of the screen itself, optimization of the parameters and correction of the effect are required.

It is usually impossible to observe the radiator at right angle, this implies depth of field issues (only part of the radiator can be focused sharply). Schiempflug solved this problem by tilting the lens in front of the camera so that all the points of the screen are focused on the plane of the sensor. This technique allows sharp images of the whole radiator, but still requires post processing to correct for the non-uniform magnification.

Optical systems are usually designed and optimised using ray tracing simulation tools, these allow the precise quantification of all sorts of aberrations. Calibration targets on the real optical system are also used to identify image distortions and tune the correction algorithms. Telecentric lenses can be used to compensate the non-uniform magnification of tilted screens.

Another important effect is the diffraction of the light in the optical system. The combination of aberrations and diffraction result in the so called point-spread-function, i.e. the size of the spot of light generated by a point source. Diffraction is well described by the Fraunhofer theory. If the point spread function is known it can be deconvoluted from the raw images increasing the sharpness.

X-Rays from synchrotron radiation are usually imaged using pinhole cameras, a trade-off between resolution and diffraction is needed for the size of the pinhole.

In some cases multiple radiations can be overlapped, e.g. scintillation and OTR. In some cases it is possible to use the different time profiles of the radiations to separate them, e.g. the OTR can be discarded if the scintillation light is acquired with a very short time delay (OTR is instantaneous while scintillation has long decay times).

Overview on camera sensor technology

Walter Tutsch, PCO, Germany

A global overview of the available solid state camera technology is presented. The common basis of all different technologies is the photodiode that collects the charges liberated by the photons. The way the charge of the photodiode is read out differs then from one technology to the other.

In CCD sensors the charge is first simultaneously shifted into a storage area, the charges of each column of the storage area are shifted one by one toward the read out register. On its turn the cells of the read out register is shifted horizontally to the ADC. In this way all the pixels are digitized by the same ADC and it is relatively easy to create a uniform response over the whole sensor area. The disadvantage is that the readout is slow and the production is costly as it requires high grade silicon. The use of high grade silicon result in low dark current so long exposures are possible.

The main CCD producer (SONY, JP) has announced the discontinuation of the CCDs production in favour of CMOS sensors in 2017. In the EMCCD the sensitivity of a standard CCD is increased by adding an electron multiplication stage (limited avalanche regime) before the output amplifier.

CMOS sensors have been around for as long as CCDs but until recently were low cost, low performance sensors used in household appliances. The technology has been improved greatly and scientific CMOS (sCMOS) sensors have now matched and surpassed the performance of the CCD. The sCMOS are based on a complex pixel design with usually 5 transistors, w.r.t. the 3 transistors of the

base CMOS design. This allows reducing the readout noise of the pixels, dominated by the thermal noise of the floating diffusion capacity, by the so called correlated double sampling technique. Readout noise of the order of 1 electron can be achieved w.r.t. the ~20 electrons of standard CMOS. High dynamic range with 16 bits digitization is also achieved in sCMOS by combining two 11 bits ADCs (a single 16 bit ADC would require too much power for an image sensor).

The complex design of the CMOS pixel reduces the silicon area available for light collection (filling factor). This effect can be reduced by using micro lenses on each pixel to focus the light on the sensitive part of the pixel or by illuminating the sensor on the back side (this requires the silicon chip to be thinned). sCMOS sensors offer high resolution, high sensitivity, high dynamic range, high frame rates, low readout noise and flexibility in the readout (multi-tap, area of interest etc.).

High resolution and high speed result in a high data rate. A new standard: "CameraLink HS" has been developed and can cope with many Gbit/s transmission in a scalable way (scalable multi-channel configuration).

Image intensifiers can be used to image very faint sources or to obtain very fast shutter times. Image intensifiers give better results when coupled to sensitive cameras, the sCMOS cameras suit perfectly this task.

CMOS and sCMOS sensors are taking over the market for image sensors and offer better performances than CCDs or EMCCD in almost all cases. The only case where CCDs are still superior is for very long exposure times thanks to the much lower dark current compared to CMOS and sCMOS.

Session 3: Cameras, Optics and Electronics II (R. Jones)

Normalization, methods and equipment for testing cameras for imaging scintillation screens

Krzysztof Chrzanowski, Inframet, Poland

This talk focused on presenting standards that would allow beam instrumentalists to correctly compare their optical systems. Although there is no standard for testing cameras for scintillation screens, the EMVA-1288 (European Machine Vision Association) standard was cited as being the most appropriate, as requirements for machine vision cameras are similar to those for imaging scintillation screens. The EMVA standard does not describe a particular set-up in detail but presents a series of recommendations for the following:

1. Measurement of sensitivity, linearity and non-uniformity using a homogeneous monochromatic light source
2. Measurement of the temperature dependency of the dark current
3. Spectral measurements of the quantum efficiency over the whole range of wavelength to which the sensor is sensitive (relative spectral sensitivity).

Inframet provides two test stations based on this standard, one for testing camera cores or imaging sensors, and another for testing complete camera systems. In addition to EMVA-1288 parameters the Inframet test stations can measure radiometric parameters (such as Noise Equivalent Illuminance/Irradiance, Non Uniformity, Signal to Noise Ratio, dead pixels and 3D Noise) as well as Imaging parameters (such as MTF, resolution, Minimal Resolvable Contrast, crosstalk, blooming and FOV). From the point of view of test equipment the type of imaging sensor does not matter, only the spectral band is important and the output interface of the electronic signal. Results were shown for the Basler acA1920 camera, which is used by many beam imaging systems.

Using such an approach, following the recommendations of the EMVA-1288 standard, would allow a fair comparison of different optical imaging systems for scintillator screens, ensuring that the quoted measurement parameters are understood to be the same.

Status and plans for beam instrumentation cameras at CERN

Enrico Bravin, CERN, Switzerland

An overview of the 200+ camera systems used at CERN for beam imaging was presented. These are still largely based on analogue cameras (CCTV type CCD, ThermoFisher CID, VIDICON) linked to a

custom-made VME frame grabber. The advantages of analogue cameras over digital cameras were cited as being:

- Having a standardised readout, making them easy to replace with different brands
- Better suited for the radiation environment of particle accelerators
- Able to easily transport the signal over long distances

However, industry is rapidly moving away from such cameras, which will make it more and more difficult to find suitable replacements in the future. CERN is therefore investigating a move to digital cameras, which provide superior sensitivity, resolution and frame-rate, but need a dedicated infrastructure for signal transport and can suffer from hardware compatibility issues due to the non-standardisation of their readout. A comparison of analogue and digital camera sensors was presented, with the superior signal to noise ($\times 4 - \times 10$) of the digital cameras clearly demonstrated.

Another topic addressed was the use of intensifiers. These are commonly used to image weak sources or to allow gating on a fraction of the beam. Intensifiers were shown to suffer from life-time issues, with examples given of photo-cathode wear and MCP degradation.

In summary CERN is being forced to move away from CCTV and VIDICON cameras, with digital GigE cameras the preferred solution, provided mitigation measures can be found to allow their use in radiation areas.

Use of imaging fibre bundles as alternative to VIDICON tubes in high radiation areas

Damiano Celeste, CERN, Switzerland

The results of direct imaging using optical fibre bundles in radiation environments were presented. It was shown that using a fibre bundle the fraction of light collected is only 2% of that of a standard optical set-up. This in itself is not an issue, as the vastly superior sensitivity of the digital camera that can be used with the fibre bundle more than compensates, when compared to a radiation hard VIDICON camera. However, the images obtained were shown to be distorted due to fibre cross-talk or light leakage in the cladding, with the exact cause still under investigation.

Radiation tests carried out at the IRMA radiation facility in Saclay (France) showed that the fibre bundle (10m of Fujikura RadHard FIGR10 – 10,000 fibres of 1.5 mm diameter) was still giving an image after irradiation up to 700 kGy. However, the degradation due to radiation was found to be non-linear across the bundle, with the outer fibres having lost up to 70 % transmission while the central fibres had only lost 30%. This is suspected to come from the different mechanical stresses that the fibres experience during production, and is something that would need to be taken into account through regular calibration if such a system were to be used for profile measurements.

Radiation tests on cameras + tests of different screens in HiRadMat

Stephane Burger, CERN, Switzerland

The results of radiation tests carried out at the CHARM facility (CERN) on 6 different BASLER digital CMOS cameras were presented. Camera failures due to single event upsets were observed after a few minutes of exposure, requiring a power cycle to resume operation. The single event probability per shot (0.005 Gy, $5E7 \text{ cm}^{-2}$ neutron equivalent fluence, $2E7 \text{ cm}^{-2}$ high energy hadron fluence) was calculated to be 11%. The digital cameras all failed irreversibly before accumulating 165 Gy. However, the response obtained from the last image before failure still had good contrast – much better than the image from an analogue camera exposed to the same radiation. Nevertheless the analogue camera was still working after accumulating 500 Gy. The conclusion was that the sensor of the digital camera is unlikely to be the cause of the failure due to radiation, and that it is more likely to be the power supply, ADC or data transfer components. For many applications at CERN the 150 Gy limit for such a camera still makes it a viable alternative to analogue cameras, provided the probability of single event failure on a single shot remains at the % level.

Asked if the manufacturer could identify which component is failing, the answer was that there was little interest from the manufacturer to look into this for such a small market. A discussion was had on whether a specifically designed camera using one of the tested sensors could be pursued. This

indeed seems like a possibility, but would require much better documentation from the sensor manufacturer, something which has been difficult to obtain up until now.

The presentation also covered the test of various screen materials at the CERN HiRadMat facility, where they were impacted by high energy density bunched beams. The tests were conducted in air, and therefore suffered from parasitic light from Cherenkov emission. Although some comparative light yield data from the various screens was presented, no precise light yield and resolution studies could be performed. There are now plans to repeat this test in a vacuum environment.

Session 4: Experiences at Proton and Ion Accelerators I (T. Lefevre)

Cameras at GSI / FAIR: Hardware – Software – Operation

Harald Bräuning, GSI, Germany

Driven by requests from the users, more and more scintillating screens have been upgraded to a digital readout in the last few years. The usage varies widely from continuous readout over many seconds with several frames per second to a single shot detection of μs long pulses triggered by machine events. Additional requirements were the simultaneous view of the images in the main control room and the experimental huts, storage of images for later analysis and measurement of beam position and approximate FWHM in SI units.

The new readout is also the prototype for scintillating screen readout in the FAIR accelerator complex, which is currently under construction. Integration into the new control system already implies a client-server architecture. The server part runs under Linux and is based on Cern's FrontEnd Software Architecture (FESA) with the client part written in Java/JavaFX. A priori, the number of clients per server is not restricted.

The standard assembly consists of a scintillating screen in a standardized holder mounted on a linear feedthrough normally driven by pressurized air. Calibration marks on the holder are used to determine the scale factors needed to convert pixel into meters. The screen is mounted under 45° with respect to the beam axis. In most, but not all, cases the camera is mounted under 90° with respect to the beam axis. The camera is equipped with a remote controlled lens. A LED is provided to illuminate the screen.

- For the camera, the UI-5240SE-M from iDS (<http://ids-imaging.com>) was chosen based on its e2v image sensor (EV76C560, <http://www.teledyne-e2v.com>). This sensor has a high sensitivity at a quantum efficiency of about 60% and a good radiation tolerance. Binning and an optional analog gain boost of factor 2 further increase the sensitivity. In addition the camera can be triggered by an external signal.
- Having a Gigabit Ethernet interface the cameras are read out by an industrial PC using a local network with a 10Gbit switch. The data acquisition software handles camera setting and image acquisition. Online processing includes cropping, rotation (90° , 180° and 270°), flipping and simple image scaling. Online analysis consists of creating projections in x and y as well as the intensity histogram. Centre-of-brightness and FWHM are calculated based on the projections without taking perspective distortions into account.
- An in-house built controller unit provides power for up to 8 cameras and the possibility to power-cycle a camera by remote command. It also distributes the trigger – initiated either by software command or by the machine timing system – to the cameras. Currently there is only one trigger for all cameras connected to a controller unit.
- The purpose of the remote controlled lenses is to adjust the image brightness via the iris. Two types of lenses are used: the Pentax -ER series and the Linos MeVis-Cm. The Pentax lens has a manual focus and an iris control by a simple DC voltage. The iris closes automatically if the voltage is cut off. The Linos lens was intended as a replacement and features a motorized iris as well as focus. Using encoders for precise and reproducible adjustment it also requires a more complex controller. Both lenses are controlled with a PLC system with the PLC controller in the electronic rooms and satellites in a radiation save area but close to the lenses. The PLC also controls the led for target illumination. Unfortunately both lenses are now discontinued.

- Recently the readout of analogue cameras like the Thermo Fischer MegaRAD3 has been implemented using the Pleora iPort Analog-Pro external frame grabber. This module is Gigabit Ethernet based and compatible with the GigE Vision and GenICam standards. As analogue cameras have a fixed frame rate, a rate reduction in software to 10Hz reduces the amount of data transported from the server to the client. In addition a software trigger is implemented by discarding all frames but the one directly following a machine event detected by the data acquisition software.
- The scintillating screen is typically mounted under 45° with respect to the optical axis. This together with the short distance between lens and screen leads to a visible perspective distortion where the scaling factor from pixels to meters is dependent on the position of the pixel itself. However, this position dependent scaling factor can be calculated based on 6 parameters obtained from the calibration marks on the standardized screen holder. While we do not rectify the image itself, these parameters are used by the client application to overlay a correct grid on top of the image, which shows the perspective correction. Using a movable cursor the application will also calculate the correct position of the pixel under the cursor in meters.

Currently we have 34 iDS cameras in operation in environments dealing with all kinds of ions, energies and intensities. So far, the operation is stable and no degradation to radiation was observed. The cameras are well supported under Linux and integrate nicely with FESA. For short pulses (few μs length) it has been observed, that the image saturates with pixel values well below the maximum value of 255. However, further investigations have not yet been possible.

Three cameras with Pleora iPort Analog-Pro frame grabbers are currently in use. They are also well supported under Linux. Some stability problems have been observed with the frame grabber stopping to send images while still being accessible by the software. Currently we assume this to be network related although all frame grabbers are in a private network. But further investigations are necessary.

Scintillating Screen Performance Measurements for 300MeV/u Ion Beams at GSI

Beata Walasek-Höhne, GSI, Germany

This talk represents the investigations in the imaging properties of inorganic scintillation screens as diagnostic elements in heavy ion accelerator facilities, which were performed at the GSI Helmholtz Centre for Heavy Ion Research and the Technical University Darmstadt. The screen materials can be classified in groups of phosphor screens (P43 and P46 phosphor), single crystals (cerium-doped $\text{Y}_3\text{Al}_5\text{O}_{12}$) and poly-crystalline aluminium oxides (pure and chromium-doped Al_2O_3). Out of these groups, a selection of seven screens were irradiated by five different ion species (proton, nitrogen, nickel, xenon and uranium), that were extracted from SIS18 in fast (1 μs) and slow (300-400 ms) extraction mode at a specific energy of 300 MeV/u. The number of irradiating particles per pulse (ppp) was varied between 10^7 and $2 \cdot 10^{10}$ ppp and the scintillation response were recorded by a standard camera system.

Two detector systems were used simultaneously to obtain the response of the scintillating material to the irradiating beam. A standard camera system provided information on the light output L , the light yield Y and the characteristics of the beam positions and profiles in horizontal and vertical direction. In parallel, a spectrometer recorded the spectral response of the materials.

Additionally analytical methods like UV/VIS transmission spectroscopy, X-Ray diffraction and Raman fluorescence spectroscopy were used after the beam times to look for changes in the material structure. Neither structural variations nor material defects, induced by the ion irradiation, were proven within the accuracy range of the used instrumentation and the given ion fluencies.

Besides the irradiation under varying beam intensities, radiation hardness tests with fast and slow extracted Ni-ion beams at $2 \cdot 10^9$ ppp were performed to study the material stability under long time irradiation. The light yield Y of the targets was nearly constant or decreased only by about 10-15 % relative to the initial value. The emission spectra remained unchanged and the beam profiles showed good accordance to the reference methods.

During all performed experiments, the targets showed a great stability. Non-linear characteristics, e.g. due to quenching during irradiation at high beam intensities, were not observed. The light yield Y showed a tendency to decrease with increasing calculated electronic energy loss dE/dx . The characteristics of the calculated beam profiles as well as the recorded emission spectra did not change significantly. So a material degradation of the investigated materials was not verified. This observation is confirmed by the performed material characterization measurements. The need of target replacement, e.g. due to damage, did not occur and was thus not performed during the complete investigations.

Radiation hardness investigations of Al_2O_3 for MeV/u ions at GSI

Peter Forck, GSI, Germany

(Summary of PhD thesis by Stefan Lederer at Technical University Darmstadt 2016)

At the GSI heavy ion LINAC with energies up to 11.4 MeV/u several screen material were investigated with the originally goal for a pepper-pot emittance measurement. A precise reproduction of the beamlet's size is fundamental for emittance calculation; in particular deformation by thermal effects and radiation damage at the beamlet's centre must be avoided. Results of those investigations for various scintillators were reported earlier; references are given in the talk. Thermal quenching has been investigated using screens equipped with an external heating system and has shown that the light yield decreases with increasing temperature as expected.

To investigate the radiation damage processes in detail, the un-doped scintillator Al_2O_3 in form a ceramic was investigated at GSI and HZDR with different ions in the energy range 0.5 to 5.9 MeV/u within a broad range of fluences up to some 10^{14} cm^{-2} . Al_2O_3 is an intrinsic scintillator, the luminescence is originated from different colour centres with maxima in the wavelength range of $\lambda = 322$ to 413 nm.

Even after radiation with a low fluence (e.g. 10^{12} cm^{-2}), the surface of the ceramic is discoloured at the beam spot; this shows the additional creation of colour centres. By annealing the original properties can be recovered. The light yield during irradiation decreases, but the rate depends significantly on the colour centre type. It was found that the F^+ centre (maximum at $\lambda = 326 \text{ nm}$) is much more radiation hard than other centres. The decreasing light yield can be described by the so called Birks model which uses macroscopic quantities (cross section and quenching ratio) to describe the damage as a function of fluence. In particular, it was shown, that the light yield by radiation damage decreases initially, but level off to an almost constant level for large fluences. This is explained by an increasing probability that a projectile induced displaced atom is stopped in a corresponding location cancelling the damage effects, i.e. doesn't lead to a net-effect. The Birks model is applied to other ceramic scintillators irradiation showing the same general behaviour, but Al_2O_3 is most radiation hard, i.e. has lowest damage cross section and low quenching ratio.

The ion induced displacements at some MeV/u ions are not attributed to nuclear stopping. The damage is caused by the large electronic stopping power (basically close to the maximum of Bethe-Bloch equation), which heats the material around the ion track and leads to amorphisation and therefore for an increasing density of colour centres. The so called thermal spike model is one possibility of describing such a process leading to the semi-empirical quantity of damage radius as a function of dose. For higher energetic ions the dose is lower, leading to less material heating around the ion track; this is confirmed by comparing the radiation damage as a function of fluence for ions in the range of MeV/u to the significantly lower damage of ions in the range of several 100 MeV/u.

Taking the radiation tolerance into account, the F^+ centre emission (maximum at $\lambda = 326 \text{ nm}$) could be used as for profile measurement by an appropriate optical filtering. Moreover, by moderate heating to e.g. $400 \text{ }^\circ\text{C}$ of the opaque ceramics with a backside heater, in-situ thermal annealing can be realized. This would enable precise profile and emittance measurements even for high beam currents.

Session 5: Experiences at Proton and ion Accelerators II (B. Walasek-Höhne)

Luminescence materials for high power targets

Cyrille Thomas, ESS, Lund, Sweden

Luminescent materials are used all over the world and in large range of application. One of them is to use luminescence properties for detecting high energy particles in high radiation environment such as high-power targets. This talk focuses on the example of imaging high power beam of particles, typically of the order of 1MW average beam power or higher, delivered to a target that can be used for instance for neutron spallation. The imaging application is highly challenging by many aspects. First of all, the requirements on the materials are strong: the luminescence yield is expected to be high, in the range of 100 thousand photons per MeV, constant and linear; it is expected to be independent from temperature variation; the fluorescence lifetime has to be less than $1\mu\text{s}$ for capturing fast events; the material lifetime has to be long enough to support operation of the accelerator.

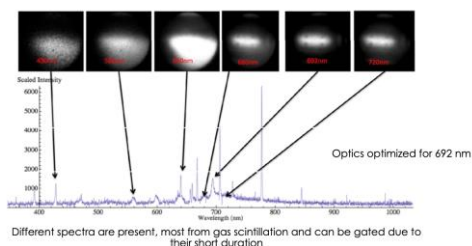
The case beam on target imaging system for the 5 MW beam at the European Spallation Source ERIC is presented in this talk. It introduces the imaging system and the imposed performance on the material. The talk presents the selected material which is similar to the material used at various facilities like for instance the CERN LHC Dump imaging system or the SNS beam on target imaging system. The properties of this material is discussed and it is shown, that in spite of not quite matching all the required performance, this material will be used for the first target and probably the next one. We also focus on the degradation aspect of the material. Irradiation studies have been carried out on this material and some of the early results are shown.

Screens from the SNS-Target

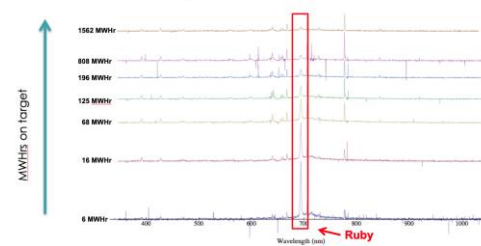
W. Blokland, SNS, Oak Ridge, USA

The spallation Neutron Source uses a $\text{Al}_2\text{O}_3:\text{Cr}$ coating on the target nose cone to see where the beam hits the target. The coating composition and spraying technique has been developed in collaboration with Stony Brook. After installation and exposure to proton beam, the coating has been tested or evaluated for: spectral response, comparison with calculated beam parameters, uniformity tests, decay in Luminescence per MWhr, effect of DPA on profile, effect of DPA on spectrum, linearity of luminescence vs beam pulse charge, duration of luminescence pulse, and calculated effect of secondary particles on luminescence. Various results are shown in Figure 1. The main issue is the loss of luminescence due to the radiation damage.

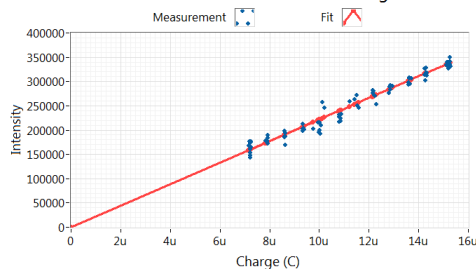
Spectral response



Effect of DPA on spectrum



Luminescence Versus Beam Charge



Prompt luminescence per proton pulse

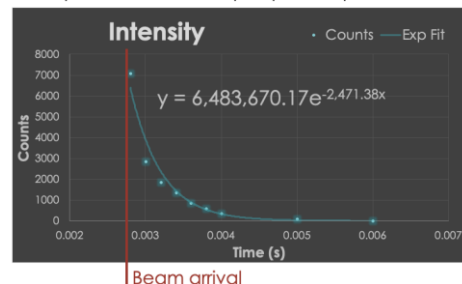


Figure 1: Various measurements performed on the SNS target coating.

The decay in luminescence per MWhr was measured but the curve was not understood. However, the Empirical Birks model (1) was given in P. Forck's talk "Radiation hardness investigations of Al₂O₃ for MeV/u ions at GSI", and this model turned out to be a good, not perfect, fit of the measured decay as shown in Figure 2. This model and other mechanisms presented at the workshop should help our understanding of the radiation damage effects.

$$S(\Phi) = S(0) \cdot \frac{1}{1+K \cdot [1-\exp(-\sigma_D \Phi)]} \quad (1)$$

with $K = \frac{k_q}{k_f + k_i}$: effect on emission as ratio between, k_q : quenching by damage i.e. displacement, k_i : internal quenching, k_f : regular luminescence emission.

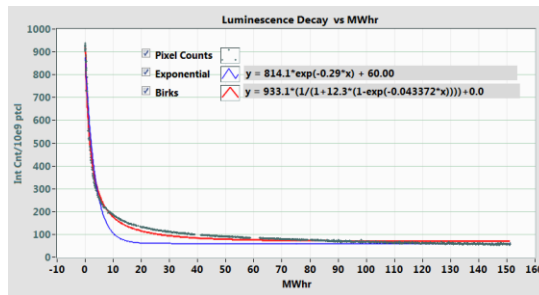


Figure 2: Fit of Birks model to the SNS Luminescence versus MWhrs of proton beam exposure.

While the current luminescent coating works for SNS, we are searching for a longer lasting brightness of the coating and will continue looking into the radiation effects and testing different coatings on our target.

Overview for RHIC complex: Screens for electrons, protons and ions

T. Miller, BNL, Brookhaven, USA

The RHIC complex of accelerators at Brookhaven National Laboratory maintains a group of five ion machines in support of nuclear research by ion collision as well as three electron machines for cooling and lensing of the ion beams. Imaging of low intensity ion beams has employed principally doped ceramic screens as well as some scintillating screens; whereas the electron machines mostly rely on monocrystalline YAG screens with some experimental nanotube screens. This presentation provides an overview of these machines and the types of screens used. Details such as optical configuration, camera systems, control topology and failure history are also covered.

Usage of scintillation screens at the medical facility HIT

H. Latzel, HIT, Heidelberg, Germany

The Heidelberg Ion Beam Therapy Center (HIT) is a medical radiation facility where cancer patients are treated with carbon ions and protons by means of a scanned pencil beams. To ensure clinically acceptable treatment conditions the position and the width of the individual pencil beams must be monitored with a precision of less than 1 mm in position deviation and $\pm 10\%$ in width. One of the three treatment rooms is the heavy ion gantry to rotate the ion beam around the patient thus using optimal beam angles. Because of the axial symmetry at the gantry it seems obvious to make use of an ion beam detector with similar symmetry. One possible implementation of such a detector is the construction of a scintillation screen in conical shape. For this reason we have set up a prototype of a conical scintillation screen to demonstrate the feasibility of this technique to measure beam position and spot size at the iso-centre within sufficient accuracy.

First results from measurements at a horizontal beam line treatment room and at the gantry show that position measurements are accurate to 0.1 mm. The reconstruction of correct beam spot sizes in the iso-centric plane from the scintillating light on the curved inner surface of the conical screen is more difficult. For all proton beam energies and low and mid-energies of the carbon beams, the results correspond to the expected spot size. At higher carbon beam energies the divergence from the expected values are bigger, thus the mathematical model still needs to be improved. The next version of the conical scintillation screen includes further optimizations of the camera, optics, and mechanical setup.

Session 6: Experiences at Electron Accelerators I (G. Kube)

Experiences with different screen material at ALBA

Ubaldo Iriso, ALBA-CELLS, Cerdanyola del Vallés, Spain

At ALBA scintillating screens are used for three different types of monitors: in conventional screen monitors where the scintillator screen interacts directly with the electron beam, as X-ray converter in In-Air X-ray detectors (IXD), and as X-ray converter for pinhole cameras. All types of monitors were covered in this contribution. Standard screen monitors for the ALBA transfer lines, linac, booster and storage ring were equipped with YAG:Ce scintillators (0.5 mm thickness, supplier Crytur), some of them additionally with OTR screens; observation geometry is 45° screen tilt angle with optics perpendicular to the beam axis. Comparative studies between OTR and YAG screen profile measurements indicated that the scintillator based beam profiles are systematically enlarged (U. Iriso et al., Proc. DIPAC'09) which was attributed to the scintillating screen thickness. Therefore linac screens were exchanged from 0.5 mm to 0.1 mm thickness, now emittance measurements agree well with OTR measurements for bunch charges typically smaller than 2 nC. Concerning IXD monitors, LYSO:Ce screens from two different suppliers were investigated (PreLude 420, Saint Gobain and CRY-19, Crytur), and it was found that the latter one had an about 30% higher light yield for 1 mm screen thickness. However, the IXD based vertical beam profiles are systematically enlarged compared to pinhole measurements which is not yet understood. For the ALBA pinhole camera measurement the observation geometry is such that the YAG:Ce scintillator (0.1 mm/0.2 mm thickness) surface normal is collinear to the X-ray beam axis with the optics being perpendicular to this axis. In view of accurate beam emittance measurements for the main storage ring the question was raised how precise absolute beam sizes could be determined: while good agreement was found for relative beam size evolution, pinhole based measurements at ALBA showed small differences compared to LOCO based calculations. It was shown that image analysis and acquisition parameters play an important role when looking at micrometer precision level. As consequence a "feedback" system will be implemented at ALBA to keep similar CCD illumination conditions.

Jefferson Lab Scintillating Screens

Kevin Jordan, Jefferson Lab, Newport News (VA), USA

A brief overview was given of the JLab accelerators, consisting of CEBAF (Continuous Electron Beam Accelerator Facility), LERF (Low Energy Recirculation Facility, former FEL), UITF (Ultimate Injector Test Facility), and GTS (Gun Test Stand). While the latter two facilities operate with YAG:Ce screens, CEBAF is equipped with 139 Chromox screens and 6 YAG screens. Due to the high failure rate of Vidicon and CCD cameras mounted close to the screens, an upgraded optics setup was designed to bring the cameras away from these radiation sources. At GTS, YAG screen damage could be observed: under UV light exposure bleaching damage became visible. The application of powder phosphor coated screens was described, having the advantage that any geometry can be spray coated using phosphor spraying techniques. As an example the FEL beam dump screen was presented. With boron nitride nano tubes (BNNT) a new scintillator material was presented, having the advantage that it is very radiation resistant and suitable for high power beam applications.

Experiments with this new material were performed for beam energies from 300 keV up to 11 GeV and first results presented.

Screen Monitors in SwissFEL

Rasmus Ischebeck, Paul Scherrer Institut, Villigen, Switzerland

Design and operation of the SwissFEL screen monitors were presented. The SwissFEL with beam energies from 5 MeV up to 6 GeV is equipped with 27 transverse profile imagers which are routinely in operation since 2016. Before finalizing the design, different cameras, scintillators (main material: YAG:Ce, supplier Crytur) and imaging geometries were tested. Design goals were operation at bunch charges between 10 and 200 pC, 10 μm resolution, 100 Hz readout, and immunity to COTR effects. The screen monitor imaging geometry is based on a geometrical optimization, described in detail in Ref. (R. Ischebeck et al., PRST-AB 18 082802), the cameras are operated in Scheimpflug geometry. Different measurement examples demonstrated the high quality which is achievable with this kind of screen monitor, as for example transverse emittance measurements and investigations of the longitudinal phase space in combination with a transverse deflecting cavity. Further applications of scintillator based beam monitors were briefly described, as the beam loss monitor system and X-ray profile monitors.

Experiences with scintillators screen at FERMI

Marco Veronese, Elettra-Sincrotrone Trieste, Italy

The 1.5 GeV seeded FERMI FEL at Elettra is equipped with about 40 screen monitors, starting from the gun up to the main beam dump. They typically consist of a combination of YAG:Ce and OTR screens. From the first bunch compressor onward, FERMI is suffering from COTR effects, therefore only scintillating screens are used in order to suppress this influence. For the intra-undulator screens a re-design was performed in order to achieve a COTR immune geometry. The achieved resolution amounted to $< 15 \mu\text{m}$ with a YAG screen thickness of 100 μm . Different applications of intra-undulator type screen monitors were presented, for example (i) the measurement of the seed laser to electron beam trajectory overlap, (ii) the seed laser pointing stability, and (iii) the imaging of the FEL radiation. For seed laser applications ($\lambda = 260 \text{ nm}$) it was demonstrated that UV scintillators (Metrolux K6) are better suited than YAG screens, for the FEL radiation measurements damage of the coating material onto YAG screens was observed. In order to be more confident, presently a new hybrid screen/wire scanner diagnostics is under commissioning. In the future, three additional screen monitor upgrades are planned, aiming mainly to increase the achievable resolution.

Session 7: Experiences at Electron Accelerators II (A.Wawrzyniak)

Scintillation screens for laser-accelerated beams

Jurjen P. Couperus Cabadağ, Helmholtz-Zentrum Dresden – Rossendorf, Germany

Scintillating screens are routinely used as beam diagnostic for electrons and proton beams originating from high-intensity short-pulse laser based novel accelerators.

In laser wakefield accelerators (LWFA), powdered rare earth phosphor ($\text{Gd}_2\text{O}_2\text{S:Tb}$) based scintillating screens are typically applied in dipole dispersive spectrometers in order to retrieve the accelerator's electron energy distribution over a large spectral range^{1,2}. The charge to photon response is calibrated for several commercially available screens. This allows them to be used for absolute charge measurements of electron beams³. A method for error-avoiding cross-laboratory implementation of these calibrations is presented. Additionally, saturation, degeneration and damage effects in long-term usage of such screens are considered.

For laser-driven ion sources (LDIS), common detection methods such as radiochromic films (RCF) and solid state track detectors (e.g., CR39) offer two-dimensional detection of the transverse angularly resolved spectrum, however do not allow for online readout. Here, two alternative scintillator based detectors offering online detection are presented. A 1D stack detector offers a high spatial resolution and energy resolution⁴. A 2D pixelated stack detector with varying absorber

thicknesses gives a slightly lower spatial resolution, but offers a full two-dimensional spatial measurement of both the beam profile and energy distribution⁵.

¹ J.P. Couperus *et al.*, *Nat. Commun.* **8**, 487 (2017)

² A. Irman *et al.*, *Plasma Phys. Control. Fusion* **60**, 044015 (2018)

³ T. Kurz *et al.*, *Rev. Sci. Instrum.* **89**, 093303 (2018)

⁴ J. Metzkes *et al.*, *Rev. Sci. Instrum.* **83**, 123301 (2012)

⁵ J. Metzkes *et al.*, *Rev. Sci. Instrum.* **87**, 083310 (2016)

Performance of a Reflective Microscope Objective and Thin Scintillator in an X-ray Pinhole Camera

Lorraine Bobb, Diamond Light Source, UK

At synchrotron light sources, X-ray pinhole cameras are commonly used to measure the transverse profile of the electron beam in the storage ring. From these profile measurements and given knowledge of the accelerator lattice, the beam emittance is calculated.

As improvements to the accelerator lattice reduce the beam emittance, e.g. with upgrades to fourth generation synchrotron light sources, likewise the beam size will be reduced such that micron and sub-micron scale resolution is required for beam size measurement. Therefore the spatial resolution (i.e. point spread function) of the X-ray pinhole camera must be improved accordingly.

In the literature it is well documented that the scintillator screen significantly contributes to the overall point spread function of the X-ray pinhole camera. To reduce this contribution, a thin scintillator screen may be used. However, a thin screen will also produce a lower photon yield.

This presentation discusses the importance of matching the scintillator screen thickness to the numerical aperture of the relay lens. For optimal spatial resolution, the performance of a thin (25 μ m) LuAg:Ce screen combined with a reflective microscope objective is compared to the nominal setup consisting of a thick (200 μ m) LuAg:Ce screen and a high quality refractive lens. The observed degradation of Prelude420 (LYSO) and LuAG:Ce screens from exposure to the X-ray beam is also presented.

Towards a bunch-resolved transverse beam-profile monitor for BESSY II and BESSY VSR

Gregor Schiwietz, Helmholtz-Zentrum Berlin, Berlin, Germany

After an introduction of the ongoing BESSY VSR project (Variable pulse-length Storage Ring) in Berlin with new hardware installations and resulting timing pattern, the corresponding requirements for beam diagnostics are discussed. These requirements lead to three new beamlines for optical and THz diagnostics at two dipole magnets. The first new diagnostic beamline is in operation since January 2019. It allows for streak-camera measurements, but also for direct beam imaging of larger profiles as well as interferometry of the vertical size by using the X-Ray baffle method.

Double-slit interferometry using visible light has already been proven at BESSY and will be installed permanently at the second diagnostic beamline. The principle for accurate horizontal as well as vertical beam-size determination with this method is presented in detail. Results are shown in comparison to existing pinhole monitors. Planned and ongoing improvements of the sensitivity of the setup are explained as well the coupling to a fast intensified CCD (ICCD) that will enable bunch-resolved interferometry for transverse beam-profiling.

Collaboration Study of Coherent Optical Transition Radiation Effects on Profile Screen Measurements

Patrick Krejcik, SLAC, Rasmus Ischebeck, PSI, Changbum Kim, PAL

Linac based FELs produce ultra-short bunches with low longitudinal emittance (energy spread). The high peak current (kiloAmps) and microbunching instability conspire to generate Coherent Optical Transition Radiation COTR at the surface of all profile monitor screen materials. The OTR becomes coherent when the microbunch length is comparable to the radiation wavelength. The COTR is both unstable and many orders of magnitude brighter, making screens unusable. We present screen

designs that mitigate this effect by directing the COTR away from the camera while preserving the optical resolution from the YAG screen using a geometry that accounts for the refraction Snell angle in the screen and the tilted Scheimpflug angle in the image plane to preserve depth of field. The influence of coherent diffraction radiation is also minimized in the latest design by arranging the internal vacuum mirrors to be further away from the beam axis. Results are presented showing the success of the design by scanning the bunch length at the LCLS beam line in the range from 1 to 10 kA peak current.

Session 8: Experiences at Electron Accelerators III (U. Iriso)

Screen Charging Effects at the European XFEL

A. Novokshono, DESY, Hamburg, Germany

The beam passing through the off-axis screen monitors causes an ionization inside the scintillator, which in this case is either LYSO or YAP with 200um thickness. The scintillator then slowly discharges, which in turn induces a Coulomb force that affects the passing of subsequent bunches and so, it affects the beam orbit and the SASE level.

Artem showed us several studies done to characterize this effect. From simulations with GEANT4, they concluded that the scintillator charge could be up to 3% of the bunch charge. On the other hand, experimental beam studies evaluated this effect into 6% of the bunch charge.

It is suspected that this disagreement might be related with a faster scintillator discharge as the expected. For this reason, further systematic studies are planned at XFEL to characterize this effect. As a possible solution, it was discussed to cover the scintillator by a conductive layer to discharge it as fast as possible.

Observation of Quenching Effects in Scintillators at the European XFEL

Gero Kube, DESY, Hamburg, Germany

The beam shape at the screen monitors at the European XFEL presented a weird “smoke-ring” shape, which resulted in a measured emittance values larger than expected. This shape was not consistent with COTR contribution or CCD saturation, and they started to look at possible causes.

Gero carefully explained the scintillation process, and modelled the electron passage inside the screen as a “straight tube” of ionization with Fermi Radius $R_F = hc/h\omega_p$. High primary (electron) beam densities results in a “quenching” of the excitation carriers, consistent with the appearance of the observed smoke-rings type shapes. For LYSO scintillators, the high density thresholds were in the order of 1nC beams into $\sigma \sim 100\mu\text{m}$.

Currently, they are also testing different screens to reduce this effect both theoretically and experimentally. Theoretically, the quest is focused on Gadolinium-based scintillators (where charge carriers rapidly transfer their energy to the excited state of Gadolinium), or YAP (where high mobility of excitation carriers reduce the quenching probability). So far, first tests with YAP and YAG showed better results than with LYSO.

Characterization of the spatial frequency response of a scintillator for beam size measurements using Heterodyne Near Field Speckles

M. Siano, University of Milano, Italy

A novel interferometric technique has been tested at the NCD-SWEET beamline at ALBA for two-dimensional beam size measurements. It relies on Fourier analysis of X-ray speckles formed by interfering the incoming radiation from an undulator with a number of spherical waves scattered by nanoparticles suspended in water.

To this aim, the spatial frequency response of the system (particle form factor and dynamics + YAG screen + relay optics) plays a fundamental role. Its effects are accounted for by introducing the Instrumental Transfer Function (ITF) in the model. It is shown how it can be characterized with the same technique and experimental setup.

Mirko shows and discusses recent results at ALBA. The measured horizontal beam size ($\sigma_h=115 \mu\text{m}$) is in good agreement with expectations (130 μm), while the vertical one ($\sigma_v=16 \mu\text{m}$) is a factor of two larger (7 μm). This discrepancy is still under study.

He finally focuses on the measured ITF. While the sample contributions can be neglected, effects of defocusing of the microscope objective with respect to the YAG screen are evidenced. Nonetheless, the ITF is well described by an exponential decay, which might be primarily dictated by the YAG. Further tests and simulations are needed to confirm this.